EFFICIENT THREE-DIMENSIONAL SIMULATION OF ULTRASOUND IMAGING USING A PARALLEL *K*-SPACE METHOD

Mohammad I. Daoud and James C. Lacefield
Department of Electrical & Computer Engineering and Robarts Research Institute
University of Western Ontario, London, Ontario, Canada
Email: mdaoud@imaging.robarts.ca

ABSTRACT

Three-dimensional (3-D) simulations of ultrasound image formation can be used to investigate quantitative relationships between characteristics of ultrasound images and the microscopic structure of tissue, which can improve tissue characterization methods. However, such simulations involve high computational complexity which limits their use in imaging research. A parallel 3-D ultrasound simulator is presented that uses an efficient numerical method to compute acoustic propagation. The simulator runs on computer clusters and enables accurate 3-D simulations with short running times. Ultrasound images of a tissue-mimicking phantom created using the simulator show realistic 3-D refraction artifacts. The parallel execution time of a simulated image using 20 cluster nodes was 18.61 hours compared to a serial execution time of 357.50 hours.

INTRODUCTION

Ultrasound imaging simulations are used to investigate quantitative relationships between ultrasound system characteristics, physical properties of tissue, and the characteristics of the image data. This should lead to improved methods of tissue characterization and automated image analysis. The core of an ultrasound imaging simulation is a numerical solution of the forward scattering problem, which is the computation of scattered and reflected waves given an incident pulse and a description of the propagation medium.

Computational complexity remains a major barrier to this research, because ultrasound imaging problems involve large-scale simulations with propagation distances on the order of hundreds of wavelengths, and hence require enormous computational resources and long running times. To perform accurate and fast three-dimensional (3-D) simulations, it is necessary to combine efficient numerical methods, which obtain high accuracy using minimal computational resources, with the use of parallel and distributed systems (PDSs).

The *k*-space methods [1] provide an attractive numerical approach to perform ultrasound imaging simulations. In these methods, spectral evaluation of spatial derivatives is combined with a temporal correction that minimizes the numerical error otherwise introduced during temporal iteration of the field. The combination of these two features permit the *k*-space methods to achieve high numerical accuracy with much coarser spatial and time steps than are needed for other numerical approaches such as finite-difference and finite-element methods. The use of coarse spatial grids and time steps reduces the computational complexity of the simulation. One formulation of a *k*-space method is the two-dimensional (2-D) algorithm developed by Tabei *et al.* [1] based on coupled first-order acoustic wave equations. In this paper, the 2-D first-order *k*-space method of [1] is extended to support 3-D ultrasound simulations.

Although the *k*-space methods use coarse temporal and spatial steps, they still require large memory and processing resources as well as long running times to carry out 3-D imaging simulations that involve multiple pulse-echo acquisitions, or scan lines. PDSs enable 3-D imaging simulations within feasible running times. One important class of PDSs is computer clusters. A computer cluster is a group of independent computers, or nodes, that communicate with each other via a communication network. The nodes of a computer cluster work together as a single integrated computing system. Computer clusters have a good performance-to-cost ratio and tend to be an accessible method of high-performance computing for most users. Therefore, this paper presents a parallel 3-D implementation of the first-order *k*-space method that runs on a computer cluster.

THEORY

In this section, the first-order *k*-space method is reviewed and formalized into three dimensions based on the derivation employed in [1] for the 2-D first-order *k*-space method.

The first-order *k*-space method solves the coupled first-order linear acoustic wave equations in a lossless fluid with spatially variable sound speed and density [2]:

$$\nabla p(r,t) = -\rho(r)\frac{\partial u(r,t)}{\partial t}$$
$$\nabla . u(r,t) = -\frac{1}{\rho(r)c(r)^2}\frac{\partial p(r,t)}{\partial t} \quad (1)$$

where $p(r,t)$ is the acoustic pressure field, $u(r,t)$ is the velocity field, $\rho(r)$ is the spatially dependent mass density, $c(r)$ is the spatially dependent sound speed, and r represents a 3-D spatial vector coordinate (x,y,z).

The spatial derivatives in (1) can be evaluated accurately using the Fourier transform [1]:

$$\frac{\partial \Phi(r,t)}{\partial \zeta} = \mathscr{F}^{-1}\{ik_\zeta \mathscr{F}\{\Phi(r,t)\}\} \quad (2)$$

where ζ denotes x, y, or z, the function $\Phi(r,t)$ can be any bandlimited signal, $\mathscr{F}$ is the 3-D spatial Fourier transform, $\mathscr{F}^{-1}$ is the inverse spatial Fourier transform, and (k_x, k_y, k_z) are the 3-D components of spatial frequency, k, defined such that $k^2 = k_x^2 + k_y^2 + k_z^2$. The assumption of bandlimited acoustic fields is justified since ultrasound pulses have bandlimited spectra. The temporal derivatives in (1) can be approximated using a finite-difference scheme:

$$\frac{\partial \Phi(r,t)}{\partial t} \approx \frac{\Phi(r,t+\Delta t/2) - \Phi(r,t-\Delta t/2)}{\Delta t} \quad (3)$$

where Δt is the time step. However, this approximation introduces significant dispersion errors.

Since each equation in (1) evaluates coupled temporal and spatial derivatives, the first-order *k*-space method uses (3) to evaluate the temporal derivative and employs a set of operators, called the first-order *k*-space operators, that accurately evaluate the spatial derivative using the Fourier transform and correct for the error introduced by the discrete evaluation of the temporal derivative. Following [1], the 3-D first-order *k*-space operators can be expressed as:

$$\frac{\partial \Phi(r,t)}{\partial^{(c_0\Delta t)^+}\zeta} \equiv \mathscr{F}^{-1}\{ik_\zeta e^{ik_\zeta \Delta\zeta/2} sinc(c_0\Delta t k/2)\mathscr{F}\{\Phi(r,t)\}\}$$
$$\frac{\partial \Phi(r,t)}{\partial^{(c_0\Delta t)^-}\zeta} \equiv \mathscr{F}^{-1}\{ik_\zeta e^{-ik_\zeta \Delta\zeta/2} sinc(c_0\Delta t k/2)\mathscr{F}\{\Phi(r,t)\}\} \quad (4)$$

where ζ denotes x, y, or z, $\Delta\zeta$ is the spatial step along the ζ-coordinate, $\mathrm{sinc}(x) = \sin(x)/x$, c_0 is the sound speed in the background medium, and $\mathrm{sinc}(c_0\Delta t k/2)$ is the temporal correction term. The exponential coefficients in (4) indicate that the *k*-space operators shift the function $\Phi(r,t)$ by half spatial steps before evaluating the spatial derivatives and applying the temporal correction terms. For instance, the operator $\partial\Phi(r,t)/\partial^{(c_0\Delta t)^-}x$ evaluates the derivative of $\Phi(r,t)$ with respect to x and applies the temporal correction term after performing a spatial shift of $-\Delta x/2$.

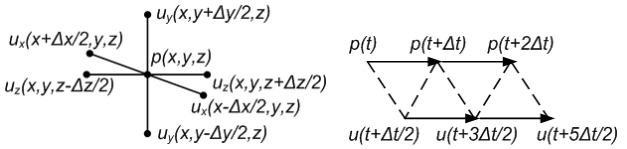

Figure 1: (a) Staggered-space and (b) staggered-time sampling configuration of the acoustic fields.

Using (3) and (4), the 3-D first-order *k*-space method equivalent to (1) can be written as:

$$u_x(r_x,t^+) = u_x(r_x,t^-) - \frac{\Delta t}{\rho(r_x)}\frac{\partial p(r,t)}{\partial^{(c_0\Delta t)^+}x}$$
$$u_y(r_y,t^+) = u_y(r_y,t^-) - \frac{\Delta t}{\rho(r_y)}\frac{\partial p(r,t)}{\partial^{(c_0\Delta t)^+}y}$$
$$u_z(r_z,t^+) = u_z(r_z,t^-) - \frac{\Delta t}{\rho(r_z)}\frac{\partial p(r,t)}{\partial^{(c_0\Delta t)^+}z} \quad (5)$$
$$p(r,t+\Delta t) = p(r,t) - \Delta t\rho(r)c(r)^2 \sum_{\zeta=\{x,y,z\}} \frac{\partial u_\zeta(r_\zeta,t^+)}{\partial^{(c_0\Delta t)^-}\zeta}$$

where $u_x(r,t)$, $u_y(r,t)$, and $u_z(r,t)$ are the x, y, and z components of the velocity field, $r_x = (x+\Delta x/2, y, z)$, $r_y = (x, y+\Delta y/2, z)$, $r_z = (x, y, z+\Delta z/2)$, $t^+ = t+\Delta t/2$, $t^- = t-\Delta t/2$, and the spatial derivatives are evaluated using the *k*-space operators. Equation (5) employs 3-D staggered-space and staggered-time schemes in which the temporal and spatial sampling of the pressure and velocity fields are configured as shown in Fig. 1. The $(c_0\Delta t)^-$ and $(c_0\Delta t)^+$ operators are combined in a way that cancels out the spatial shift between the terms of each difference equation in (5) and satisfies the sampling layout of the acoustic fields. This *k*-space method enables an exact temporal iteration without dispersion errors for homogeneous propagation media, i.e. $\rho(r) = \rho_0$ and $c(r) = c_0$, and provides high accuracy for weakly scattering media such as soft tissue [1].

Following the procedure applied to the 2-D *k*-space method of [1], frequency-dependent absorption is incorporated into the 3-D first-order *k*-space method using an Nth-order relaxation model [3]. In this model, the compressibility is written as:

$$\kappa(r,t) = \kappa_\infty(r)\delta(t) + \sum_{i=1}^{N}\frac{\kappa_i(r)}{\tau_i(r)}e^{-t/\tau_i(r)}H(t) \quad (6)$$

where $\kappa_\infty(r)$ is the compressibility as frequency approaches infinity and it is taken here to be $1/[\rho(r)c(r)^2]$, $\tau_i(r)$ is the relaxation time for the ith-order relaxation process, $\kappa_i(r)$ is the modulus for the the ith-order relaxation process, $\delta(t)$ is the Dirac delta function, and H(t) is the Heaviside step function. Absorption is implemented in the *k*-space method by additional equations that model artificial fields with time- and position-dependent state variables. The number of additional

equations depends on the complexity of the absorption model. Our implementation of the 3-D *k*-space method incorporates relaxation process absorption using two relaxation processes, i.e. N in (6) is equal to 2, and six additional equations.

METHODS

Parallel implementation

For ultrasound imaging simulations that require computation of many independent scan lines, serial evaluation of the 3-D first-order *k*-space method requires long running times. To reduce the running time of a simulation, a parallel implementation of the 3-D *k*-space method is developed to enable fast simulations using computer clusters [4]. This parallel implementation is achieved by dividing the simulation grid of each scan line among a group of cluster nodes such that each node applies the *k*-space method iteratively on its locally assigned grid points. Multiple groups of nodes are used to compute independent scan lines concurrently.

Numerical accuracy evaluation

The incident pulse used to evaluate the accuracy of the 3-D *k*-space method and the B-mode imaging simulations described in the next section has a Gaussian envelope, a center frequency of 40 MHz, and -6-dB bandwidth of 24 MHz. This is a typical pulse used for small-animal imaging in preclinical research.

The accuracy of the *k*-space method was evaluated using a benchmark test in which the scattered field from a fluid sphere of diameter 0.24 mm is computed and compared with an analytical plane-wave solution [5]. The sphere has the acoustic properties of human fat ($c = 1.478$ mm/μs and $\rho = 0.950$ g/cm^3) [1] and is embedded in a water background at body temperature ($c = 1.524$ mm/μs and $\rho = 0.993$ g/cm^3) [1]. The total pressure field is recorded at 45 observation points located in the forward scattered direction on a line 0.48 mm in length perpendicular to the propagation direction. The accuracy is measured using the L^2 error [1] between the pressure signals recorded at the observation points using the *k*-space method and the analytical solution, respectively. The accuracy results are reported for thirteen Courant-Friedrichs-Lewy (CFL) numbers [1] varying between 0.1 and 1.3 with an increment of 0.1 with the spatial step fixed at 4 points per minimum wavelength, where the maximum frequency of the incident pulse is taken as 70.9 MHz. The CFL number relates the time step to the spatial step such that CFL $= \frac{c_0 \Delta t}{\Delta x}$.

The performance of frequency-dependent absorption is tested by propagating the incident pulse in a medium with sound speed and density of water at body temperature. The parameters of the two relaxation processes, which are optimized to approximate an absorption coefficient of 0.05 dB/cm/MHz, are given by: $\kappa_1 = 4.85 \times 10^{-4} \kappa_\infty$, $\tau_1 = 4$ ns, $\kappa_2 = 4.51 \times 10^{-4} \kappa_\infty$, and $\tau_2 = 40$ ns. The incident pulse is propagated using a spatial step size of four points per minimum wavelength and two CFL numbers: 0.25 and 0.5. The simulated frequency-dependent absorption is measured and compared with an analytical formula of relaxation absorption as a function of frequency [3].

B-mode imaging simulations

An example B-mode imaging simulation is carried out using a tissue-mimicking phantom to demonstrate the feasibility of the 3-D parallel *k*-space method for imaging studies with short execution times. The phantom is composed of an infinite-length cylinder of diameter 1.7 mm with acoustic properties of connective tissue stroma ($c = 1.550$ mm/μs and $\rho = 1.040$ g/cm^3) [6] containing two internal spheres of diameters 0.5 and 0.4 mm with acoustic properties of human fat and surrounded by a background medium with acoustic properties of water at body temperature. The axis of the cylinder is aligned along the z-axis and the centers of the spheres are located on the xy plane ($z = 0$). The incident pulse is transmitted along the y direction from a highly-focused spherical transducer with a 0.47 mm diameter, a 1.23 mm focal length, a focus located on the xz plane ($y = 0$), and the same center frequency and bandwidth as the previous simulations; the same transducer is used to receive the backscattered waves. The characteristics of the modeled transducer are chosen to approximate the lateral spatial resolution and depth of field of a 40 MHz transducer used in a commercial high-frequency ultrasound system [7]. A set of parallel B-mode image planes are obtained at various z coordinates, where each image is composed of 65 scan lines that are equally-spaced by 40 μm along the x direction. The simulation of each scan line is carried out using a computation grid of $128 \times 512 \times 128$ points, a spatial step of 5 μm, and a time step of 1.64 ns. Each B-mode image is computed using 20 nodes, such that the first 60 scan lines are simulated by allocating two nodes for each line, while the simulation of the last five scan lines is performed by using four nodes for each scan line.

RESULTS

Numerical accuracy

Accuracy results for the 3-D first-order *k*-space method obtained using the sphere benchmark problem are presented in Fig. 2(a) as a function of CFL number. The *k*-space method achieves high accuracy for CFL numbers below 0.5; however, the error values increase gradually as the time-step size increases for CFL numbers greater than 0.5. For the range of CFL numbers

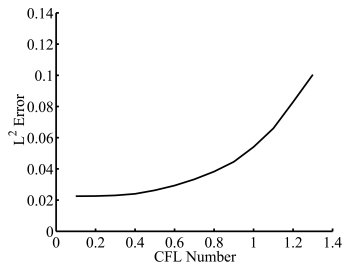

(a)

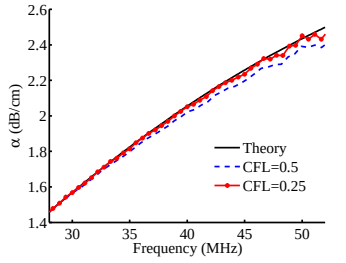

(b)

Figure 2: (a) L^2 error of the 3-D *k*-space method as a function of CFL number. (b) Performance of the relaxation absorption model.

examined in this study, the *k*-space method did not suffer from any numerical instability. The high accuracy and stability of the *k*-space method enables the use of coarse spatial and time steps while achieving accuracy higher than other comparable methods.

The performance of frequency-dependent absorption is shown in Fig. 2(b) for a range of frequencies within -40 dB from the central frequency component in the incident pulse spectrum. The absorption as a function of frequency obtained using CFL numbers of 0.5 and 0.25 is very close to the theoretical frequency-dependent absorption [3]. However, the numerical accuracy of frequency-dependent absorption at high frequencies that is obtained using a CFL number of 0.25 is better than the accuracy achieved with a CFL number of 0.5. For example, relative error at 50 MHz reduced from 1.9% to 0.7% by using a CFL number of 0.25 instead of 0.5.

B-mode imaging simulations

The simulated B-mode images for the tissue mimicking phantom are shown in Fig. 3, where each panel presents a B-mode image plane obtained at different elevations along the z-axis. The B-mode images show realistic 3-D refraction artifacts that appear as shadow regions with reduced brightness located below the spherical lesions. Such 3-D artifacts cannot be obtained using 2-D simulations. The serial execution time required to compute each image was 357.50 hours, compared to the parallel execution time of 18.61 hours using 20 nodes.

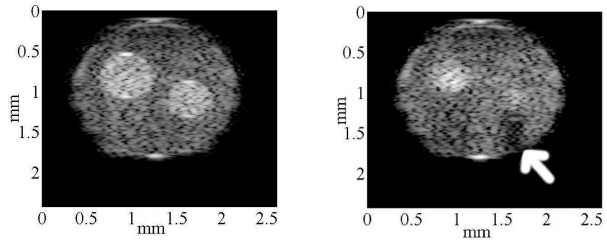

(a) (b)

Figure 3: Simulated B-mode images of a tissue-mimicking phantom containing spherical lesions acquired when the focus of the transducer is located at $x = 0$, $y = 0$, and (a) $z = 0$ mm and (b) $z = 0.2$ mm. Panel (b) contains a shadow region with reduced brightness indicated with a white arrow.

ACKNOWLEDGMENT

The authors thank Dr. Makoto Tabei, Dr. T. Douglas Mast, and Prof. Robert C. Waag for providing the source code for the serial 2-D *k*-space software and Ge Baolai for technical assistance. This research was supported by Natural Sciences and Engineering Research Council (NSERC) Discovery Grants 261323-03 and 261323-07. Mohammad I. Daoud is a Scholar of the Canadian Institutes of Health Research/University of Western Ontario Strategic Training Initiative in Cancer Research and Technology Transfer and holds an NSERC PGS-D scholarship. The results reported in this paper were obtained using the computing facilities of SHARCNET.

REFERENCES

[1] M. Tabei, T. D. Mast, and R. C. Waag, "A *k*-space method for coupled first-order acoustic propagation equations," *J. Acoust. Soc. Am.*, vol. 111, pp. 53–63, 2002.

[2] A. D. Pierce, "The wave theory of sound," in *Acoustics: An Introduction to Its Physical Principles and Applications*, 2nd Edition, Acoustical Society of America, Woodbury, NY, 1989, ch. 1.

[3] A. I. Nachman, J. Smith, and R. C. Waag, "An equation for acoustic propagation in inhomogeneous media with relaxation losses," *J. Acoust. Soc. Am.*, vol. 88, pp. 1584–1595, 1990.

[4] M. I. Daoud and J. C. Lacefield, "Parallel three-dimensional simulation of ultrasound imaging," *submitted to 22nd International Symposium on High Performance Computing Systems and Applications*, 2008.

[5] P. M. Morse and K. U. Ingard, "The scattering of sound," in *Theoretical Acoustics*, McGraw-Hill, New York, NY, 1968, ch. 8.

[6] S. W. Huang and P. C. Li, "Ultrasonic computed tomography reconstruction of the attenuation coefficient using a linear array," *IEEE Trans. Ultrason. Ferroelectr. Freq. Control*, vol. 52, pp. 2011–2022, 2005.

[7] F. S. Foster, M. Y. Zhang, et al, "A new ultrasound instrument for in vivo microimaging of mice," *Ultrasound Med. Biol.*, vol. 28, pp. 1165–1172, 2002.